Layer double hydroxide and sodium montmorillonite multilayer coatings for the flammability reduction of flexible polyurethane foams

You-Hao Yang, Yu-Chin Li, John Shields, Rick D. Davis

National Institute of Standards and Technology, Engineering Laboratory, 100 Bureau Drive MS-8665, Gaithersburg, Maryland 20899-8655
Correspondence to: R. D. Davis (E-mail: Rick.Davis@NIST.gov)

ABSTRACT: Flexible polyurethane foam (PUF) is coated by layer-by-layer (LbL) assembly using branched polyethyleneimine (BPEI), poly (acrylic acid) (PAA), and two different charged nanoparticles, such as sodium montmorillonite (Na-MMT) and layered double hydroxide (LDH). Three different deposition strategies, that is, bilayer, trilayer, and quadlayer, exhibit different coating growth, morphology, and flammability properties. Changing the nanosheet from LDH to Na-MMT dramatically alter the coating mass for the same number of layers. A five bilayer PAA/BPEI+LDH coating reduced the peak heat release rate by 40% and the average heat release rate by 70%, which is two times more effective than commercial fire retardants (FRs) and other LbL-FR coatings for PUF. Na-MMT and LDH mixed multilayers resulted in effective flame-retardant coatings with less coating mass by manipulating the deposition strategy. This study manifests the flexibility of LbL to fine-tune flammability reduction by switching the coating weight gains, which is significant to accelerate the development of other LbL coating regardless of the intended applications. © 2014 Wiley Periodicals, Inc. J. Appl. Polym. Sci. 2015, 132, 41767.

INTRODUCTION

In 2010, there were 366,600 home fires causing 2,570 civilian fire fatalities, 13,210 fire injuries, and $7.2 B in direct damages.[1] This represents a cost of more than $32 B annually.[2] Flexible polyurethane foam (PUF) is the primary cushioning material used in soft furnishings (upholstered furniture and mattresses). PUF is extremely flammable and is the reason soft furnishing fires result in the largest number of household fire fatalities and injuries.[3]

A novel approach to increase the fire resistance of PUF is to create a fire-blocking coating using layer-by-layer (LbL) assembly. By submersing a substrate (e.g., PUF) into positively and negatively charged polyelectrolyte and/or nanoparticle solutions, a positive–negative pairing layer, called a bilayer (BL), will adhere to the surface by electrostatic attractions.[4–6] Other forces have also been used to promote LbL-coating growth, such as hydrogen bonds,[7,8] covalent bonds[9,10], and donor/acceptor interactions.[11,12] Besides fire-resistant coatings[13,14], this technology has been used for gas barriers,[15,16] antimicrobials,[17,18] and electrically conductive coatings.[19,20]

Flame-resistant LbL coatings were first reported by Jamie Grunlan's group at Texas A&M (2009). [21] Using branched polyethylenimine (BPEI) with laponite on cotton fabrics, a 10

BPEI/laponite BL coating resulted in a 6% residue char at 500°C.[21] Grunlan's group later reported an improvement of 7% to 13% residue char at 500°C using a sodium montmorillonite (Na-MMT)-based formulation.[22] More recently, Chang et al reported a 72% reduction in the peak heat release rate of cotton fabric using a BPEI/diammonium phosphate and urea coating produced by a continuous dipping LbL process.[23]

In addition to textiles, LbL fire-resistant coatings have also been applied on polyurethane foam. Li et al. reported that a 4.8% mass BPEI/PAA/Na-MMT trilayer LbL coating produced a peak heat release rate (pHRR) reduction on 30%.[24] Kim et al. reported that by combining both polymer and nanoparticles in the same depositing solution to produce a faster and more fire-resistant coating. The five BL BPEI/(PAA+Na-MMT)$_{pH=2}$ coating produced a 42% reduction in pHRR.[25] This was the first time the LbL coating fire performance was evaluated in full-scale fire tests. Compared to a standard furniture foam, this BL-coated foam caused a 53% reduction in the pHRR. Other examples include, Carosio et al.[26] reported a 55% reduction in pHRR using a pure polymer chitosan-based QL coating, Laufer et al.[27] reported a 52% reduction in pHRR using a pure polymer chitosan and poly(vinyl sulfonic acid) BL coating, and Li
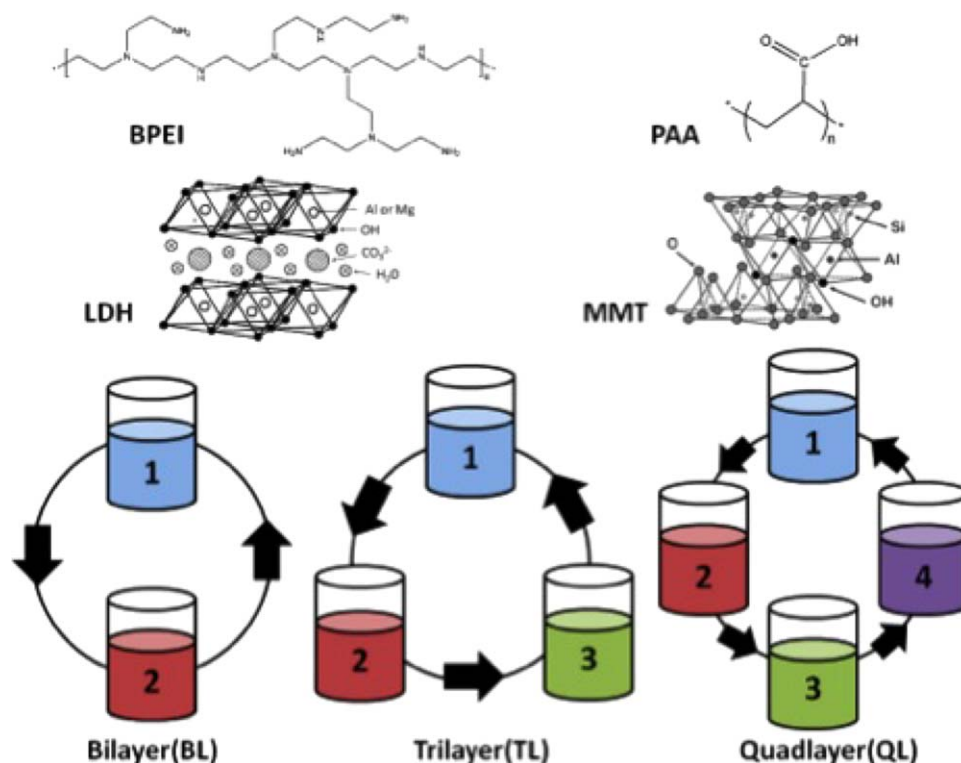
Figure 1. Schematic of the bi-, tri-, and quadlayer layer-by-layer coating sequences and of the compounds used in the coatings. The structure of LDH is revised from a previous publication.[36] [Color figure can be viewed in the online issue, which is available at wileyonlinelibrary.com.]

et al.[28] reported a 51% reduction using a chitosan, DNA, and Na-MMT BL coating.

LDH is a two-dimensional nanomaterial consisted of brucite-like cationic metal oxides layers (e.g., magnesium and aluminum oxide) and balancing by intercalated anions.[29] The major flame-retardant characteristic of LDH is its endothermic decompositions with the formation of water vapor and metal oxide residue.[30] The water vapor dilutes the combustible gas, and the solid-phase residue acts as a gas and thermal barrier to impede the supply of volatile gas and oxygen to flame and heat to the matrix. In recent years, LDH has been applied as effective nano-filler in various polymer matrixes for flammability reductions. Costache *et al.* reported a 33% reduction in poly(methyl methacylate) pHRR by using 7% sodium 4-styrenesulfonate–modified LDH.[31] Costache *et al.* later reported pHRR reductions for various polymer–LDH nanocomposites: 55% for polyethylene, 39% for ethylene vinyl acetate, and 35% for polystyrene.[32] Alongi *et al.* also used the hydrotalcite, LDH with inorganic sheets of Mg and Al, as a surface coating on the cotton fabric, and reported 20 s delay in time to ignition and 30% reduction in pHRR.[33] Carisio *et al* also reported the LDH coating with commercial polyester fabrics with 60 s delay in time to ignition and 26% reduction in pHRR. [34]

Li *et al.* previously reported LDH-based LbL coatings produce a more effective fire resistance coating than Na-MMT-based analogs.[35] The PAA/LDH/BPEI 2 TL coating reduced the pHRR by41%. Compared to previous conventional Na-MMT-based coatings, this LDH-based coating produced a (1) better flammability reduction using less fabrication steps [24] or (2) similar

flammability reduction, but with lower coating mass and less fabrication steps. [25]

In this research, we are attempting to produce a rapidly forming fire resistance coating for PUF by combining both LDH and Na-MMT in different LbL constructions (i.e., BL, TL, and QL). LDH and Na-MMT are oppositely charged. This allows us to produce coatings where both can be incorporated in adjoining monolayers so that every monolayer contains one of these protective layer forming nanoparticles. The polymer binders are BPEI and PAA, which alone have no intrinsic fire retardancy, but form rapidly growing and effective LbL fire-retardant coatings when combined with Na-MMT or LDH.

EXPERIMENTAL

Unless otherwise indicated, all materials were used as-received, all % values are mass %, and all data are reported with a 2σ uncertainty.[36,37]

Materials

Branched poly(ethyleneimine) (BPEI) (Aldrich, St. Louis, MO) ($M_W = 25,000$ g/mole) was dissolved into 18.2 MΩ deionized (DI) water to create a 0.2% cationic solution. Poly(acrylic acid) (PAA) (Aldrich, St. Louis, MO) ($M_W = 100,000$ g/mole) was dissolved into DI water to create a 0.2% anionic solution. Sodium montmorillonite (Na-MMT) (trade name: Cloisite NA+) (Southern Clay Inc., Gonzalez, TX) was dispersed in DI water with 0.5% and 1.0% to create anionic mixtures. Layered double hydroxide (LDH) (trade name: Perkalite LD-20SL) (Akzo Nobel Chemicals GmbH, Conlogne, Germany) was also

dispersed in DI water with 0.5% and 1.0% to create cationic mixtures. The chemical structure of each ingredient using in this study are shown in Figure 1. Water purified in a Millipore system was used during all the experiments. Standard (untreated) polyurethane foam was received from FXI Inc. (Media, PA) and was stored as-received from the supplier. The density of the foam is 29.1 kg/m³, and it was cut into (10.2 × 10.2 × 5.1 ± 0.1) cm for coating and cone fire testing.

Layer-by-Layer Deposition

A schematic of the LbL deposition is shown in Figure 1. Polyurethane foams (PUF) were pretreated by soaking in a $0.1M$ nitric acid solution for 5 min. This increased the PUF surface charge density, which promoted coating growth. For a bilayer (BL) coating, the pretreated PUF was submersed, squeezed several times, and left to soak in a negatively charged polyelectrolyte solution (PAA, Na-MMT or PAA+Na-MMT) for 5 min. The PUF was removed, the excess solution was squeezed back into the depositing container, and then, the PUF was rinsed with DI water. The PUF was then submersed, squeezed several times, and left to soak in a positively charged polyelectrolyte solution (BPEI or BPEI+LDH) for 5 min. The PUF was removed, the excess solution was squeezed back into the depositing container, and then, the PUF was rinsed with DI water. This completed the depositing on 1 BL. This BL sequence was repeated until the desired number of layers was achieved with the only difference being a 1-min soak instead of a 5-min soak. The coated PUF was dried in a convection oven at 70°C ± 3°C overnight and then stored in a desiccator for one day before further characterization or testing. To determine coating mass gain, water was first removed by storing the PUF in a dessicator for at least one day before coating and after coating. The mass difference (measured using a laboratory microbalance) is the coating mass gain.

The trilayer (TL) and quadlayer (QL) coatings were prepared using this procedure, except there was one additional layer in the TL sequence and two additional layers in the QL sequence. For the TL coating, the PUF was submersed in PAA, BPEI+LDH, and then Na-MMT solutions to create the PAA/BPEI+LDH/Na-MMT coatings. For the QL coating, the PUF was submersed in PAA, LDH, BPEI, and then Na-MMT solutions to create the PAA/LDH/BPEI/Na-MMT coatings.

Coating Characterization

Mass gain of LbL coatings were measured by a QCM200 quartz crystal microbalance (QCM) Digital Controller and a QCM25 crystal oscillator (Standard Research System Inc., Sunnyvale, CA). A 5 MHz Cr/Au crystal was first primed with a PEI layer by dipping into 0.1% PEI solution for all four systems, and then, coatings were deposited following the same sequence as described for the PUF. The mass change was calculated by the Sauerbrey equation, $\Delta f = -C_f \times \Delta m$, Where Δf represents the frequency change, C_f represents the sensitivity factor for the crystal and Δm represents the change in mass per unit area in g/cm².

A Zeiss Ultra 60 Field Emission-Scanning Electron Microscope (FE-SEM, Carl Zeiss Inc., Thornwood, NY) was used to acquire surface specimens of the coatings on the PUF under a 5 kV accelarating voltage. All SEM samples were sputter coated with 8 nm of Au/Pd (60%/40% by mass) prior to imaging.

Fourier transform infrared spectroscopic (FTIR) spectra of coated foams and neat LDH and Na-MMT powders were measured with a TENSOR 27 spectrometer (Bruker Optics Inc, Billerica, MA) operating in attenuated total reflectance (ATR) mode equipped with a ZnSe single crystal. The samples were scanned 64 times with a resolution of 4 cm^{-1} over the wave numbers ranging from 4000 cm^{-1} to 600 cm^{-1}.

The residues of PUF, uncoated and coated foams, were measured with a TG 449 F1 Jupiter® Thermogravimetric analyzer (TGA, Netzsch, Burlington, MA). A 10 mg specimen was isothermed at 90°C for 30 min, and then, the temperature was increased at 20°C/min to 850°C under air atmosphere. The residual mass of each coated PUF is LDH and/or Na-MMT. This mass was used to calculate the mass of these nanoparticles in the coatings. A description of the calculations is provided in Supporting Information (eqs. S1 through S5). The TGA curves are provided in Supporting Information (Figure S3).

Flammability Testing

A dual-cone calorimeter (35 kW/m² with an exhaust flow of 24 L/s) following the standard protocol defined in ASTM E1354-07 is used for measuring the foam flammability. The substrate was placed in a pan constructed using aluminum foil with only the top of the specimen exposed to the cone heater. The standard uncertainty is ±10% in heat release rate (HRR) and ±2 s in time. Average and total heat release rate values (aHRR and THR) are calculated between 0 s and the time at which the HRR values are at least 5 kW/m² and stay below 5 kW/m² for 15 s.

RESULTS AND DISCUSSION

In this research, we are attempting to produce a rapidly forming fire resistance coating for PUF by combining LDH and Na-MMT in different LbL constructions (i.e., BL, TL, and QL). LDH and Na-MMT are oppositely charged, which enables them to be incorporated in different layers of the same coating construction sequence. We assumed that this should produce a highly nanoparticle-filled coating with higher fire resistance using less number of layers than previously reported for LbL fire-resistant coatings on PUF.

Eight different coatings were investigated in this study (Table I). All the coatings contained PAA and BPEI produced from depositing solutions containing 0.2% of the polymer. All the coatings contained one or both of the LDH and Na-MMT nanoparticles. The nanoparticles were either combined with a polymer in the same depositing solution (e.g., T1) or were in a separate depositing solution (e.g., Q1). The nanoparticle concentration in the depositing solution was either low (0.5%) or high (1.0%). There were three coating sequences used in this study, which only differ in the number of layers that constitute the coating repeat sequence (i.e., 2 for BL, 3 for TL, and 4 for QL). All coatings were fabricated using five applications of the depositing sequence; therefore, the number of monolayers to produce the coating increases with number of monolayers that constitute a coating sequence (e.g., 5 BL is 10 monolayers, whereas 5 QL is 20 monolayers).

Table I. List of All the Deposition Recipes and Weight Gain on Polyurethane Foams

Id	Coating sequence	Deposit solution (Mass %)				Weight gain (%)
		PAA	LDH	BPEI	Na-MMT	
B1	PAA/BPEI+LDH	0.2	0.5	0.2	–	25
B2	PAA/BPEI+LDH	0.2	1.0	0.2	–	30
B3	PAA+Na-MMT/BPEI	0.2	–	0.2	0.5	11
B4	PAA+Na-MMT/BPEI+LDH	0.2	0.5	0.2	0.5	11
T1	PAA/BPEI+LDH/Na-MMT	0.2	0.5	0.2	0.5	11
T2	PAA/BPEI+LDH/Na-MMT	0.2	1.0	0.2	1.0	7.5
Q1	PAA/LDH/BPEI/Na-MMT	0.2	0.5	0.2	0.5	13
Q2	PAA/LDH/BPEI/Na-MMT	0.2	1.0	0.2	1.0	8.4

The uncertainty is ± 2% of the reported values

Coating Growth and Characterization

To form an effective fire resistant coating on foam using LbL, the coatings must add at least 5% to the foam mass and contain at least 20% of a char former nanoparticle (typically Na-MMT). All of the coating formulations satisfied both criteria. The LDH bilayers (B1 and B2) produced a 25% to 30% coating, which is in the range where we can expect to have very good fire resistance with a nanoparticle-based LbL coating on PUF. Replacing LDH with Na-MMT (B3) and using both LDH and Na-MMT (B4) caused the coating mass to decrease by more than half (11% coating mass). When compared to previously reported LDH TL coatings (HH5 and HL5)[35], these B1 and B2 BL required less number of coating monolayers (10 as compared to 15) and a depositing solutions with lower polymer concentration (0.2% as compared to 0.5%) to achieve a similar coating mass gain (∼25%). In accordance with coating growth, it is suggested that the PAA/LDH+BPEI BL is more efficient than PAA/LDH/BPEI TL.

In an attempt to increase the coating mass into the 30% range, the nanoparticles were into their own depositing solutions (T1, T2, Q1, and Q2), as this might promote a stronger interaction between PAA and BPEI, which has been shown to produce coatings that grow at exponential rates.[38] Unfortunately, this had the same impact as adding Na-MMT to the BL coatings. The TL coating with the Na-MMT separated out (T1 and T2) and the QL with both LDH and Na-MMT separated (Q1 and Q2) increased the coating mass by 7% to 13% with the lower increase resulting from the lower nanoparticle concentration depositing solutions. When compared to previously reported LDH TL coatings (LL5 and LH5), these Q1 and Q2 QL coatings had five additional layers but delivered a lower coating mass. (≈ 8% as compared to ≈ 15%).[35] These additional layers in the QL are Na-MMT. This suggests that these extra Na-MMT monolayers are restricting interdiffusion of BPEI and PAA.

It is assumed that the relationship between the coating mass and the formulations is primarily based on the extent of polymer interdiffusion between the monolayers. BPEI and PAA coatings grow at exponential rates due to the strong interdiffusion of the polymer chains between the monolayers created by these low-charge density polymers (i.e., high pH for BPEI and low pH for PAA solutions).[38,39] In this study, the polymer-depositing solutions were at the natural pH values (10.5 for

BPEI and 3.2 for PAA). Adding LDH or Na-MMT had no impact of the pH of these solutions. Therefore, these solutions were at a pH for which exponential coating growth could be expected. The slow coating growth is then attributed to nanoparticles in the deposition solutions that limit polymer interdiffusion, which has been reported by others.[13,24,40,41] This restricted interdiffusion is perhaps more severe in the coatings with individual nanoparticle monolayers (e.g., TL and QL).

QCM was used to help understand what part of the deposition sequence impacted coating growth (Figure 2). B2, T2, and Q2 sequences were chosen to investigate the placement of the nanoparticle. In general, the growth was similar through the first five coating sequences. Beyond the fifth repeat, T2 and Q2 are similar and continue to grow at the same linear rate. However, B2 diverts growing at a much fast rate. This suggests the Na-MMT monolayer in the T2 and Q2 may be restricting coating growth, perhaps by restricting polymer interdiffusion.

SEM and ATR-FTIR (supporting information) were used to access the quality (e.g., the extent of coverage) of the FR coatings. In more than 100 SEM images, the coatings appeared similar to those provided in Figures 3 and 4. All of the PUF internal and external surfaces were completed covered with a rough, scaly coating. SEM images of B1, T1, and Q1 clearly show the existence of LDH on the surface. B3 (no LDH)
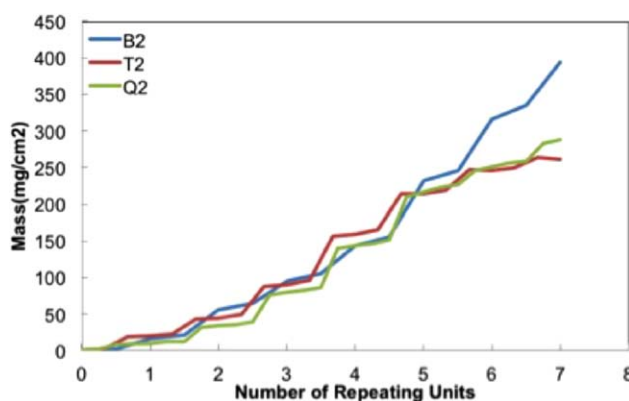
Figure 2. QCM measured mass as a function of repeating units deposited. The mass uncertainty is ± 5% of the reported values. [Color figure can be viewed in the online issue, which is available at wileyonlinelibrary.com.]
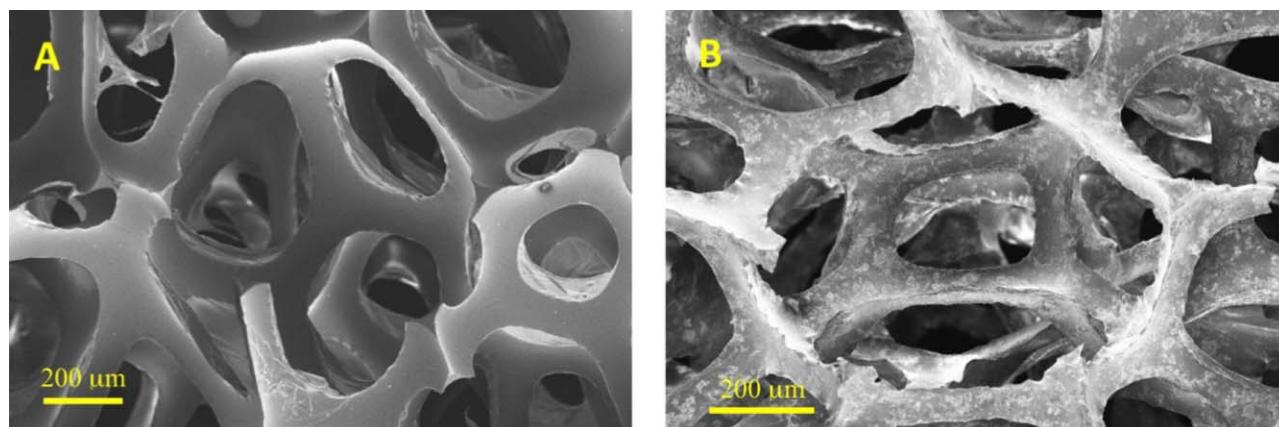
Figure 3. SEM surface images of the PUF control (A) and Q1 (B) coated foams. [Color figure can be viewed in the online issue, which is available at wileyonlinelibrary.com.]

exhibits a slightly smoother surface, perhaps because the Na-MMT platelets are significantly larger than LDH. At higher magnification, this size difference becomes more prevalent.

Flammability Testing

The cone calorimeter (cone) is a commonly used instrument to measure the bulk flammability characteristics of materials. The sample is exposed to an external heat flux, which forces the material to undergo pyrolysis. When sufficient fuel (pyrolysis products) is produced, ignition occurs and the sample undergoes combustion and continues to pyrolyze. The most common parameters reported from the test are time to ignite (TTI), maximum amount (peak) of heat released during the test (pHHR), time after ignition to reach the pHRR (t-pHRR), total amount of heat released during the test (THR), and average

amount of heat released during the test (aHRR). Cone data and HHR curves for the starch-based coatings are provided in Figure 5 and Table II. The HRR curves are grouped by the type of coating sequence (BL, TL, and QL).

Thermal gravimetric analysis (TGA) was used to determine the amount of residue produced from thermally degrading coated and uncoated foam. Except for the differences in the amount of residue, the TGA curves (mass % vs. time) were nearly identical for all formulations (supporting information). The residue was primarily nanoparticles, and therefore, the residue mass and coating mass were used to calculate the amount of nanoparticles in the coating (Table II). The equations for calculating nanoparticle content from the residue and the actual TGA curves are provided in Supporting Information
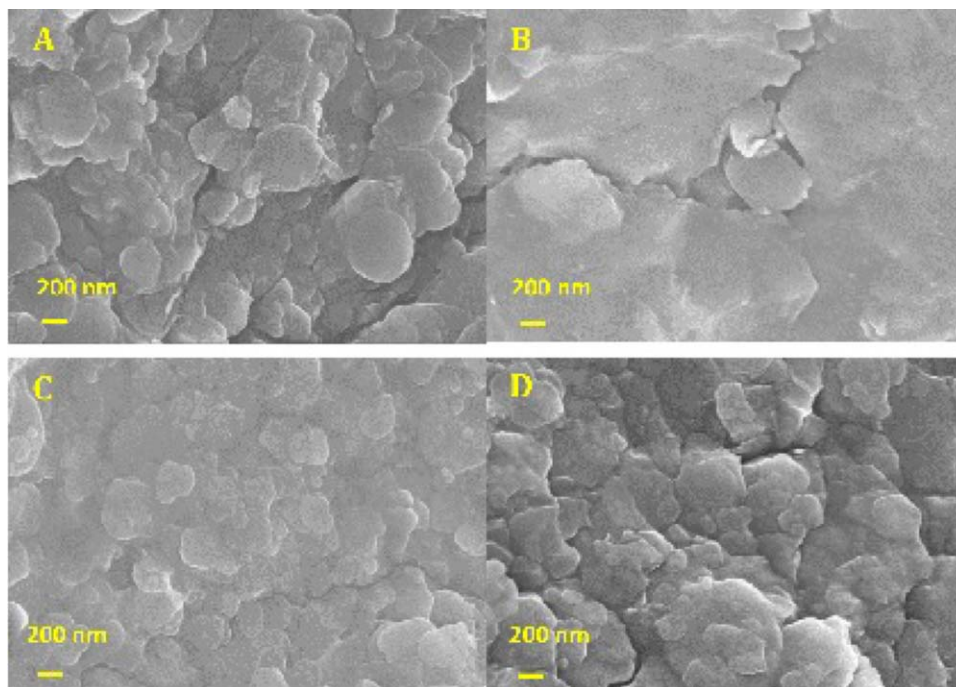
Figure 4. SEM surface images of coated PUF. (A) B1, (B) B3, (C) T1, and (D) Q1. All of them are imaged at 30,000x. [Color figure can be viewed in the online issue, which is available at wileyonlinelibrary.com.]
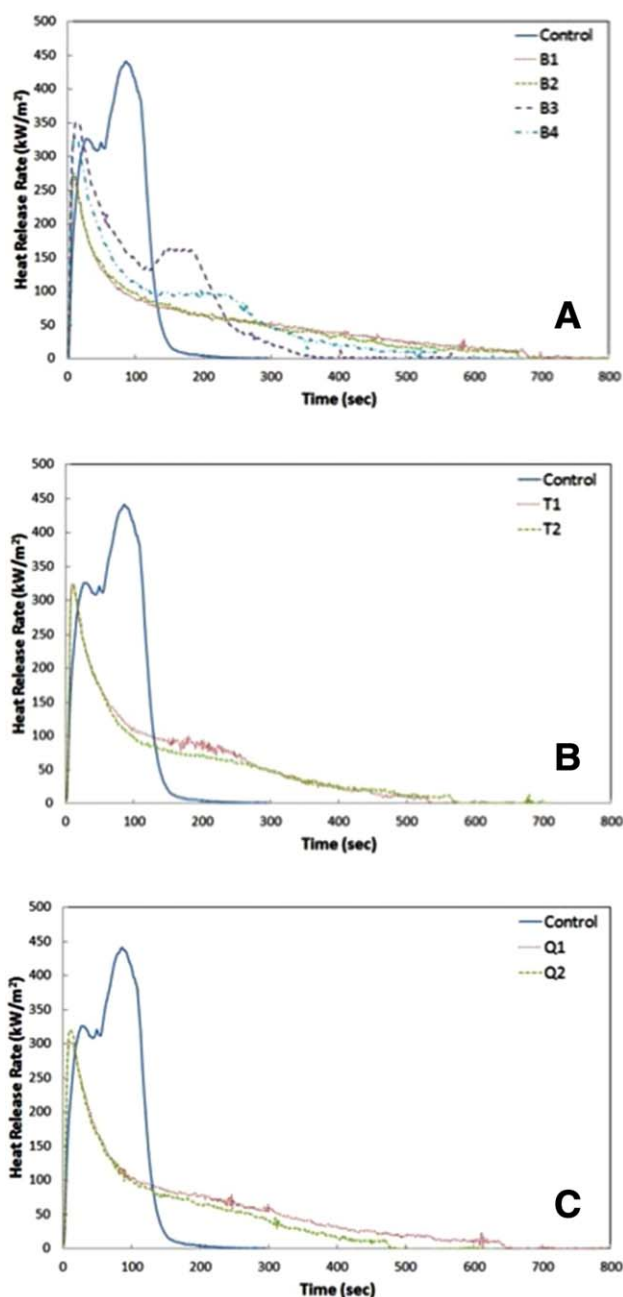
Figure 5. Heat release rate curves of control and (A) BL-, (B) TL-, and (C) QL-coated foams. The uncertainty is ±10% in HRR and ±2 s in time. [Color figure can be viewed in the online issue, which is available at wileyonlinelibrary.com.]

(eqs. S1 through S5, and Figure S3, respectively). We are unable to use the residue to calculate nanoparticle content for coatings that contain both LDH and Na-MMT because the calculation assumes that the ratio of LDH to Na-MMT is known. Therefore, we approximated the nanoparticle content by assuming that the residue contains Na-MMT and LDH in equal proportion (based on the coating formulations).

The PUF (control) exhibited typical combustion behavior in the cone (Figure 5 and Table II). The heat release rate curve (HRR) consists of two peaks associated with the combustion polyurethane

decomposition products; polyisocyanate (337 kW/m^2 ± 34 kW/m^2), and polyol (451 kW/m^2 ± 45 kW/m^2).[42] The latter is the pHRR reported for PUF. PUF is completely consumed very quickly (154 s) releasing a total heat (THR) of 43 MJ/m^2. The average amount of heat released during PUF combustion is 275 kW/m^2.

All of the FR coatings significantly reduced the flammability of the PUF. In general, the reductions are in the range of 20% to 40% for pHRR, 50% to 70 % for aHRR, and 10% to 20% for THR. Except for B3 and B4, the HRR curves had only one sharp peak. The protective layer was formed quickly and was very effective at slowing down combustion, as observed by the rapid decrease in HRR after the peak and the low and plateau-like HRR for the remainder of the fire test.

The eight coatings fall into three pHRR reduction categories; about 20%, 30%, and 40 %. The largest reduction (40%) came from the BL coatings only containing LDH (B1 and B2). These coatings also produced a 69% reduction in aHRR and about 17% reduction in THR in average. The LDH TL (LH2) previously reported produced the same pHRR reduction and aHRR reduction, but only required one-third of the coating mass.[35] It cannot be believed that TL performs better than the BL reported here, because both previous research[35] and B1/B2 showed that there is no further impact on pHRR and aHRR at more than 10% LDH coating. We believe that the flammability reduction of B1 and B2 will be maintained even at a lower coating mass (e.g., 10% to 15%).

Replacing LDH (B1 and B2) with Na-MMT (B3) decreased the magnitude of the pHRR and aHRR reduction to 22% and 33%, respectively. This improvement with LDH is consistent with previous research that showed a LDH TL (PAA/LDH/BPEI) produced the same pHRR and aHRR reduction (42% and 71%) as the best Na-MMT LbL coating (PAA+Na-MMT/BPEI BL), but only required one-third of the coating mass.[35] The better flammability performance of B1 and B2 as compared to B3 is likely not due to difference in coating mass as we believe LDH would yield the same performance even at a coating mass comparable to B3 asdiscussed earlier. There are two explanations for the better performance. One explanation is the Na-MMT content is low (32% for Na-MMT as compared to about 56% for LDH) (Table II). In general, lower mass coatings require higher nanoparticle content to achieve a similar flammability reduction as a higher mass coating. Another explanation is LDH is a better fire-retardant nanoparticle. Both Na-MMT and LDH enhance the formation of a protective char. However, LDH releases water and goes through an endothermic decomposition of the metal hydroxide layers, which causes a cooling effect that slows the combustion process.[30]

Regardless of the coating sequence, combining both Na-MMT and LDH in a single coating (B4, T1, T2, Q1, and Q2) resulted in a flammability reduction that was better than Na-MMT only, but not as good as LDH only. The pHRR and aHRR reductions were comparable for all the LDH/Na-MMT coatings (about 30% and 60%, respectively). For the LDH-only coatings, these reductions were 39% and 69%, respectively. In order to achieve similar reduction values for the LDH/Na-MMT formulations,

Table II. Impact of FR Coatings on Cone Characterized Flammability and Nanoparticle Content in the FR Coatings

ID	Coating mass %	Nanoparticle in the coating (%)	Flammability reduction			Residual mass %
			pHRR	aHRR	THR	
PUF	–	–	451 kW/m^2	275 kW/m^2	43 MJ/m^2	–
B1	25	54	271 (40%)	84 (69%)	37 (14%)	18.8
B2	30	58	275 (39%)	84 (69%)	35 (19%)	19.4
B3	11	32	351 (22%)	184 (33%)	43 (0%)	6.5
B4	11	32	329 (27%)	120 (56%)	40 (7%)	7.1
T1	11	43	324 (28%)	111 (60%)	39 (9%)	8.6
T2	7.5	64	320 (29%)	111 (60%)	36 (16%)	11.8
Q1	13	29	303 (33%)	100 (64%)	41 (5%)	10.9
Q2	8.4	56	312 (31%)	119 (57%)	34 (21%)	18.6

The uncertainty is ±2% of the reported reduction, coating mass, and nanoparticle on the coating values. The uncertainty is ±10% of reported the pHRR, aHRR, and THR values
Numbers in parenthesis represent the percent reduction.

more coating layers must be deposited. Recall all of the formulations were fabricated using 5 repeats of the coating sequence. Therefore, we suggest all formulations could achieve a similar flammability reduction, but using the mixed LDH/Na-MMT formulations requires more fabrication steps to do so (e.g., 2 to 5 more repeats of the coating sequence).

The primary application of this coating technology is low flammability foam to manufacture fire-resistant furniture. In this study, we did not conduct full-scale fire validation tests of furniture containing foam with these LDH/Na-MMT fire-resistant coatings. In a previous publication[43], we demonstrated a strong relation between the decrease in heat release (flammability) caused by Na-MMT-based coatings on foam (cone data) and furniture containing the Na-MMT-coated foam (full-scale furniture calorimeter). Based on this study, in full-scale fire tests, it is believed that the relative performance of these different formulations will be consistent with the relative ranking in accordance with the cone data. More specifically, in full-scale furniture fire tests, the expected fire reductions are as follows: LDH only (B1 and B2) > LDH and Na-MMT (B4, T1, T2, Q1, and Q2) > Na-MMT only (B3).

Residue Characterization
During cone testing, PUF foam collapses almost immediately to form a pool-like fire. After the test, there was only a discolored stain on the bottom of the aluminum pan. Na-MMT-based LbL-coated foams formed a protective residue that reduced the extent of the foam collapse. In the best cases, the Na-MMT post-test samples had similar dimensions to the starting foam and consisted of a black and a brittle powder-like residue. There was no evidence of polyurethane remaining after the cone tests. LDH-based LbL fire-retardant coated foams retained much of the foam original dimensions, and there was significant amount of polyurethane detected throughout the post-test sample.[35] This suggested the protective coating was of sufficiently high quality that it caused the fire to extinguish prior to consuming all of the polyurethane fuel.

B1 appears very similar to previous reports of LDH-based TL FR coating on PUF (Figure 6).[35] The top third of the sample is black and a brittle powder, except the top surface is a fine white powder (LDH). The middle third is also black in color, but there is a hint of yellow, and it has some structural integrity. The bottom third is yellow-orange, sticky and also had some structural integrity. The yellow is believed to be molten polyurethane that has cooled down and solidified after the last. The amount of residual polyurethane increases from top to bottom.

The post-test residues for T1 and Q1 are similar to Na-MMT-based LbL FR coating on PUF. The entire residue is black and brittle. However, the color is lighter (more gray) than Na-MMT-based LbL coatings. We believe that this is attributed to LDH, which produces white inorganic oxides when degraded.

Figure 6. Postcone images of (A) B1, (B) T1, and (C) Q1. [Color figure can be viewed in the online issue, which is available at wileyonlinelibrary.com.]

CONCLUSION

Fire-resistant coatings on PUF were constructed using nanoparticles (LDH and/or Na-MMT) and three different coating sequences (bilayer, trilayer, and quadlayer). Switching between these types of nanoparticles and coating sequences allowed precise control of the coating mass gain, nanoparticle content, and flammability reduction of PUF. The flammability reductions are in the range of 20% to 40% for pHRR, 50% to 80% for aHRR, and 10% to 20% for THR. All the coatings were constructed of five repeating sequences (5BL, 5TL, and 5QL). The coatings increased the PUF mass by 8% to 30% and contained 30% to 60% nanoparticles. The largest flammability reduction (40%) came from the LDH BL coatings (B1 and B2). Replacing LDH with Na-MMT produced the lowest flammability reduction (20%, B3). Using both Na-MMT and LDH (B4, T1, T2, Q1, and Q2), regardless of the repeat sequence, produced a flammability reduction between these single nanoparticle-type coatings. Future studies will include evaluation of these coatings on full-scale upholstered furniture fire tests.

ACKNOWLEDGMENTS

REFERENCES

1. Ahrens, M. Home Structure Fires; National Fire Protection Association: Quincy, MA, **2013**.

2. Morgan, A. B.; Gilman, J. W. *Fire Mater.* **2013**, *37*, 259.

3. Zammarano, M.; Kramer, R. H.; Harris, R.; Ohlemiller, T. J.; Shields, J. R.; Rahatekar, S. S.; Lacerda, S.; Gilman, J. W. *Polym. Adv. Technol.* **2008**, *19*, 588.

4. Lvov, Y.; Decher, G.; Mohwald, H. *Langmuir* **1993**, *9*, 481.

5. Cheung, J. H.; Stockton, W. B.; Rubner, M. F. *Macromolecules* **1997**, *30*, 2712.

6. Decher, G.; Schlenoff, J. B. Multilayer Thin Films: Sequential Assembly of Nanocomposite Materials 2nd ed..; Wiley-VCH: Weinheim, **2012**.

7. Stockton, W. B.; Rubner, M. F. *Macromolecules* **1997**, *30*, 2717.

8. Sukhishvili, S. A.; Granick, S. *Macromolecules* **2002**, *35*, 301.

9. Tian, Y.; He, Q.; Tao, C.; Li, J. B. *Langmuir* **2006**, *22*, 360.

10. Bergbreiter, D. E.; Liao, K. S. *Soft Matter.* **2009**, *5*, 23.

11. Wang, H. P.; He, Y. N.; Tuo, X. L.; Wang, X. G. *Macromolecules* **2004**, *37*, 135.

12. Benten, H.; Ogawa, M.; Ohkita, H.; Ito, S. *Adv. Funct. Mater.* **2008**, *18*, 1563.

13. Kim, Y. S.; Harris, R.; Davis, R. *ACS Macro Lett.* **2012**, *1*, 820.

14. Li, Y. C.; Mannen, S.; Morgan, A. B.; Chang, S. C.; Yang, Y. H.; Condon, B.; Grunlan, J. C. *Adv. Mater.* **2011**, *23*, 3926.

15. Yang, Y. H.; Bolling, L.; Priolo, M. A.; Grunlan, J. C. *Adv. Mater.* **2013**, *25*, 503.

16. Laufer, G.; Kirkland, C.; Cain, A. A.; Grunlan, J. C. *Carbohydr. Polym.* **2013**, *95*, 299.

17. Chiono, V.; Carmagnola, I.; Gentile, P.; Boccafoschi, F.; Tonda-Turo, C.; Ballarini, M.; Georgieva, V.; Georgiev, G.; Ciardelli, G. *Surf. Coat. Technol.* **2012**, *206*, 2446.

18. Dvoracek, C. M.; Sukhonosova, G.; Benedik, M. J.; Grunlan, J. C. *Langmuir* **2009**, *25*, 10322.

19. Park, Y. T.; Ham, A. Y.; Yang, Y. H.; Grunlan, J. C. *RSC Adv.* **2011**, *1*, 662.

20. Li, Y.; Chen, S. S.; Wu, M. C.; Sun, J. Q. *Adv. Mater.* **2012**, *24*, 4578.

21. Li, Y. C.; Schulz, J.; Grunlan, J. C. *ACS Appl. Mater. Interfaces* **2009**, *1*, 2338.

22. Li, Y. C.; Schulz, J.; Mannen, S.; Delhom, C.; Condon, B.; Chang, S.; Zammarano, M.; Grunlan, J. C. *ACS Nano.* **2010**, *4*, 3325.

23. Chang, S. C.; Slopek, R. P.; Condon, B.; Grunlan, J. C. *Ind. Eng. Chem. Res.* **2014**, *53*, 3805.

24. Li, Y. C.; Kim, Y. S.; Shields, J.; Davis, R. *J. Mater. Chem. A.* **2013**, *1*, 12987.

25. Kim, Y. S.; Li, Y. C.; Pitts, W. M.; Werrel, M.; Davis, R. D. *ACS Appl. Mater. Interfaces.* **2014**, *6*, 2146.

26. Carosio, F.; Di Blasio, A.; Cuttica, F.; Alongi, J.; Malucelli, G. *RSC Adv.* **2014**, *2*, 16674.

27. Laufer, G.; Kirkland, C.; Morgan, A. B.; Grunlan, J. C. *ACS Macro Lett.* **2013**, 361.

28. Li, Y. C.; Yang, Y. H.; Kim, Y. S.; Shields, J.; Davis, R. *Green Mater.* **2014**, *2*, 144.

29. Li, L.; Ma, R. Z.; Ebina, Y.; Iyi, N.; Sasaki, T. *Chem. Mater.* **2005**, *17*, 4386.

30. Costa, F. R.; Wagenknecht, U.; Heinrich, G. *Polym. Degrad. Stabil.* **2007**, *92*, 1813.

31. Costache, M. C.; Wang, D. Y.; Heidecker, M. J.; Manias, E.; Wilkie, C. A. *Polym. Adv. Technol.* **2006**, *17*, 272.

32. Costache, M. C.; Heidecker, M. J.; Manias, E.; Camino, G.; Frache, A.; Beyer, G.; Gupta, R. K.; Wilkie, C. A. *Polymer* **2007**, *48*, 6532.

33. Alongi, J.; Tata, J.; Frache, A. *Cellulose* **2011**, *18*, 179.

34. Tata, J.; Alongi, J.; Frache, A. *Fire Mater.* **2012**, *36*, 527.

35. Li, Y. C.; Yang, Y. H.; Shields, J.; Davis, R. *Polymer* **2014**.

36. Wang, X. M.; Ding, H. M.; Shan, Y. K.; He, M. Y. *Chn. Chem. Lett.* **2004**, *15*, 1227.

37. Mendelsohn, J. D.; Barrett, C. J.; Chan, V. V.; Pal, A. J.; Mayes, A. M.; Rubner, M. F. *Langmuir* **2000**, *16*, 5017.

38. Yang, Y. H.; Haile, M.; Park, Y. T.; Malek, F. A.; Grunlan, J. C. *Macromolecules* **2011**, *44*, 1450.

39. Yang, Y. H.; Bolling, L.; Haile, M.; Grunlan, J. C. *RSC Adv.* **2012**, *2*, 12355.

40. Podsiadlo, P.; Michel, M.; Lee, J.; Verploegen, E.; Kam, N. W. S.; Ball, V.; Lee, J.; Qi, Y.; Hart, A. J.; Hammond, P. T.; Kotov, N. A. *Nano Lett.* **2008**, *8*, 1762.

41. Priolo, M. A.; Gamboa, D.; Holder, K. M.; Grunlan, J. C. *Nano Lett.* **2010**, *10*, 4970.

42. Pitts, W. *Fire Technol.* **2011**, 1.

43. Kim, Y. S.; Li, Y. C.; Pitts, W. M.; Werrel, M.; Davis, R. D. *ACS Appl. Mater. Inter.* **2014**, *6*, 2146.